Turkish Journal of Electrical Engineering & Computer Sciences

http://journals.tubitak.gov.tr/elektrik/

Research Article

Turk J Elec Eng & Comp Sci
(2020) 28: 956 – 968

doi:10.3906/elk-1906-143

Adaptive prescribed performance servo control of an automotive electronic throttle system with actuator constraint

Zitao SUN, Xiaohong JIAO*
School of Electrical Engineering, Yanshan University, Qinhuangdao, Hebei, P.R. China

Received: 23.06.2019 • **Accepted/Published Online:** 27.11.2019 • **Final Version:** 28.03.2020

Abstract: To further improve the transient and steady-state performance of automotive electronic throttle position tracking, in this paper an adaptive prescribed performance servo control strategy is designed and applied to a real electronic throttle control system. In view of the possible high gain of the prescribed performance controller in practice, the actuator constraint is also considered in the controller design. The designed servo controller can ensure the transient and steady-state responses of tracking error are limited in the range prescribed by the performance function, and converge with the prescribed convergence rate and have no overshoot. The incorporated adaptive updating law can enhance the robustness of the transient and steady-state performance against uncertainty from the product tolerance, the operating conditions, and the aging of components. Both Matlab/Simulink simulation and dSPACE-based hardware-in-the-loop experimental verification show the effectiveness and applicability of the proposed control strategy.

Key words: Automotive electronic throttle, position tracking, prescribed performance, adaptive technique

1. Introduction

As a core part of an engine, the electronic throttle control system (ETCS) plays an important role in vehicle control because it affects the engine's operating efficiency. Therefore, fast and accurate response to the command signals of the ETCS can improve vehicle drivability, fuel economy, and emissions performance. However, the performance of an ETCS is greatly affected by nonlinearity from friction, gear backlash, and return spring, and uncertain physical parameters caused by different working conditions, production tolerances, and aging of components. Consequently, control strategy research that addresses these issues is always a popular topic in automotive engine control.

In the past few years, many control strategies-such as adaptive control [1–5], sliding control [6–8], fuzzy control [9–11], and finite-time convergence control [12, 13]-have been applied in the automotive ETCS to achieve fast dynamic response and strong robust performance against nonlinearities and uncertainties. Therefore, an adaptive technique is popular because less knowledge of the plant is required. In addition, the controller can be implemented without time consuming experiments for precise characterization of the system's dynamics and there is no need for the controller to be customized for just a single product. Consequently, the integration of various control approaches with an adaptive technique have received considerable attention. For example, compound control of a PID-type feedback controller and feed-forward compensator with an adaptive updating law are widely used, which was designed by Pavcovic et al. [3] based on identification for the principle part and self-tuning for some process parameters. In Jiao et al. [1], the adaptive update law is introduced into whole

*Correspondence: jiaoxh@ysu.edu.cn

servo tracking control including a feedforward compensator, nonlinearity compensator, and PID-type feedback controller. The adaptive technique is also often combined with sliding mode control [6–8]. The adaptive inverse model technique is adopted in radial basis function (RBF) neural networks in Yuan et al. [5], discrete-time model reference adaptive control is presented in Montanaro et al. [2], and the adaptive backstepping recursive technique is integrated into the framework of finite-time stability theory in Jiao et al. [12].

When applying the advanced control strategy in a practical system, the saturation constraint is also a very important control problem. When a stricter control performance is required, it will be more likely for high gain of the control input to appear. When the designed controller is implemented in practice, this often produces control-signal saturation due to the physical restriction of the actuator. This saturation problem will potentially affect the control performance of the real system, resulting in system performance degradation or even loss of stability if mishandled. In view of these facts, some theoretical studies have been published on control strategies dealing with the input saturation problem, such as by Chen et al. and Wen et al. [14, 15]. The theoretical results have been applied in handling the input saturation of various practical systems [6, 16, 17].

In the present paper, considering the crucial transient requirement of the ETCS, a particular performance bound technique, as presented by Han and Lee [18] and utilized in many practical systems (e.g., robots [19] and servo mechanisms [20]) will be applied in the tracking controller design for a throttle valve opening. The control strategy is derived by integrating the adaptive backstepping recursive technique into the framework of prescribed performance control for an electronic throttle with actuator constraint. The selection of the performance function in the prescribed performance control can give the ETCS a quick and no-overshoot transient response, while simultaneously the tracking error is between the upper and lower limits of the performance function during the entire system operation. The real-time adjustment of the adaptive laws for uncertain parameter estimations can ensure the robustness of the control performance of the system under different working conditions, aging, and production deviations.

2. Automotive electronic throttle system

A schematic of the ETCS is shown in Figure 1. When the reference plate position is obtained by trade-off between the driver request (acceleration pedal position) and the effective traction possibilities depending on drivability, safety, and emission, the ECU generates a pulse width modulation (PWM) signal according to the desired plate position θ_r and the actual opening signal θ drives a DC motor. The driving force of the DC motor through the reduction gearbox, the spring force, and friction of the reverse spring causes the throttle plate to flip and remain stable at the desired position. Then the position sensor transmits the current opening signal back to the ECU. Thereby, the closed loop control system of the electronic throttle is formed. According to the mechanical and electrical characteristics of the ETC, the dynamic equation of the system is as follows:

$$\begin{cases} L\dot{i}_a = u - Ri_a - K_e\omega_m \\ J_m\dot{\omega}_m = K_t i_a - B_m\omega_m - T_m \\ J_t\dot{\omega} = T_l - B_t\omega - T_f(\omega) - T_{sp}(\theta) - T_L \end{cases} \tag{1}$$

Here u is the control voltage. i_a is the armature current. ω_m and ω are the angular velocities of the motor and throttle plate, respectively. T_L is the load torque including the disturbance torque caused by the effect of air flow force acting on the throttle plate. T_m and T_l are the input and the output torques of the gearbox, respectively. Assume that there is no loss during transmission and the backlash is neglected, the gearbox transmission model is $T_l(t) = nTm(t)$. The friction torque T_f and the return-spring torque T_{sp} are

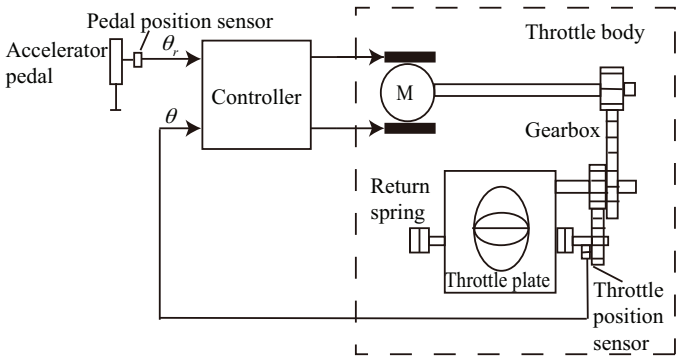

Figure 1. Schematic of the electronic throttle control system.

described as

$$T_f(\omega) = F_c\text{sgn}(\omega), \quad T_{sp}(\theta)=T_{LH}\text{sgn}(\theta-\theta_0)+k_s(\theta-\theta_0), \theta_{min}\leq\theta\leq\theta_{max},$$

where $\text{sgn}(\cdot)$ is the sign function. The notations of the physical parameters are shown in Table 1.

Table 1. Notations of physical parameters.

Symbol	Meaning of the symbol	Unit
R	Armature resistance	Ω
L	Armature inductance	H
K_e	Electromotive force constant	$\text{V}\cdot\text{s/rad}$
K_t	Motor torque constant	Nm/A
J_m, J_t	Motor, throttle equivalent moment inertial	$\text{kg}\cdot\text{m}^2$
B_m, B_t	Motor, throttle equivalent viscous damping	$\text{Nm}\cdot\text{s/rad}$
n	Gear ratio	/
F_c	Coulomb friction coefficient	Nm
T_{LH}	Spring offset	Nm
k_s	Spring gain	Nm/rad
θ_0	Default opening of the throttle plate	rad
$\theta_{min}, \theta_{max}$	Minimum, maximum allowed plate position	rad

Considering the input saturation constraint $-U_{\max} \leq u(t) \leq U_{\max}$, define

$$u(v(t)) = \begin{cases} U_{\max} & \text{if } v(t) > U_{\max} \\ v(t) & \text{if } -U_{\max} \leq v(t) \leq U_{\max} \\ -U_{\max} & \text{if } v(t) < -U_{\max}, \end{cases} \tag{2}$$

where $U_{\max}$ is a known constant and $u(v(t))$ denotes the plant input subject to saturation type nonlinearity.

Moreover, the small value of L can be ignored. The return spring may cause asymmetric behavior of the viscous damping B_t during acceleration and deceleration [4]. Therefore, the dynamic model used in the control

strategy design is modified as

$$\begin{cases} \dot{\theta} = \omega \\ b\dot{\omega} = -a_1\theta - a_{2^+}\left(\frac{1+\mathrm{sgn}(\omega)}{2}\right)\omega - a_{2^-}\left(\frac{1-\mathrm{sgn}(\omega)}{2}\right)\omega + a_3 - a_4\mathrm{sgn}(\theta-\theta_0) - a_5\mathrm{sgn}(\omega) + u(v(t)) - \bar{T}_L, \end{cases} \tag{3}$$

where $a=\frac{R}{nK_t}$, $a_1=ak_s$, $a_{2^{+,-}}=aB+nK_e$, $a_3=a_1\theta_0$, $a_4=aT_{LH}$, $a_5=aF_c$, $b=aJ$, $J=n^2J_m+J_t$, $B=n^2B_m+B_t$, and $\bar{T}_L=aT_L$.

It can be seen from (3) that the existence of nonlinear factors such as reverse spring and friction will cause viscous sliding and hysteresis, which increase the difficulty in controlling the desired opening of the valve. In addition, it is worth noting that for a real electronic throttle, due to different operating conditions, different manufacturing process requirements, product error, and mechanical damage aging, the system's physical parameters are not completely known, and there will be some degree of uncertainty, especially k_s, θ_0, T_{LH}, and F_c. Load torque T_L is also an uncertain variable. Therefore, to ensure the throttle angle θ tracking the desired trajectory θ_r with the required transient and static tracking performance, the prescribed performance control technique is introduced to satisfy the following control specifications in the controller's design.

(i) The adjustment time is required to be less than 100 ms for any operating conditions and reference signal changes. Meanwhile, no overshoot should be present in the step response. Furthermore, the throttle plate shall never hit the mechanical end stroke [1].

(ii) The average value of the steady-state tracking error is not larger than 0.11 deg [1].

(iii) The tracking error $e(t)$ is between the upper and lower limits of the performance function:

$$\rho(t) = (\rho_0 - \rho_\infty)e^{-\lambda t} + \rho_\infty, \tag{4}$$

where ρ_0, ρ_∞, and λ are positive constants defined appropriately [18]. Furthermore, for no overshoot, it is required that $0<e(t)<\rho(t)$ if $e(0)>0$, and $-\rho(t)<e(t)<0$ if $e(0)\leq 0$, and the steady-state error $e_{ss}\leq\rho_\infty$.

(iv) The designed controller should conform to physical constraints on control input and safety.

3. Adaptive prescribed performance servo control strategy design

For the system (3) with the uncertain parameters and input saturation constraint, an adaptive prescribed performance servo controller is designed as

$$v=\hat{b}\ddot{\theta}_r+\hat{a}_1\theta+\hat{a}_{2^+}\left(\frac{1+\mathrm{sgn}(\omega)}{2}\right)\omega+\hat{a}_{2^-}\left(\frac{1-\mathrm{sgn}(\omega)}{2}\right)\omega-\hat{a}_3+\hat{\bar{T}}_L+\hat{a}_4\mathrm{sgn}(\theta-\theta_0)+\hat{a}_5\mathrm{sgn}(\omega)-\hat{b}\dot{\alpha}+\frac{\xi(t)}{\varphi(t)}+k_2z+k_3(z-\eta) \tag{5}$$

with the adaptive updating laws

$$\begin{cases} \dot{\hat{a}}_1 = \frac{1}{r_1}z\theta, \quad \dot{\hat{a}}_3 = -\frac{1}{r_4}z, \quad \dot{\hat{a}}_{2^+} = \frac{1}{r_2}z\left(\frac{1+\mathrm{sgn}(\omega)}{2}\right)\omega, \quad \dot{\hat{a}}_{2^-} = \frac{1}{r_3}z\left(\frac{1-\mathrm{sgn}(\omega)}{2}\right)\omega \\ \dot{\hat{a}}_4 = \frac{1}{r_5}z\mathrm{sgn}(z), \quad \dot{\hat{a}}_5 = \frac{1}{r_6}z\mathrm{sgn}(\omega), \quad \dot{\hat{b}} = \frac{1}{r_7}z(\ddot{\theta}_r - \dot{\alpha}), \quad \dot{\hat{\bar{T}}}_L = \frac{1}{r_8}z \end{cases} \tag{6}$$

and the virtual control law α and the transformation of error ξ are chosen as follows:

$$\alpha = (\dot{\varphi} - k_1\varphi)\xi, \ \xi(t) = e(t)/\varphi(t), \ z = \dot{\theta}_r - \omega - \alpha, \ e(t) = \theta_r - \theta \tag{7}$$

$\varphi(t)$ is a piecewise continuous function defined as the following form, which is related to the tracking error $e(t)$:

$$\varphi(t)=\begin{cases}\rho(t), & e(t)\geq 0\\ -\rho(t), & e(t)<0\end{cases} \tag{8}$$

and η is the state variable of the auxiliary design system used to reduce the saturation effect [6]:

$$\dot{\eta}=\begin{cases}-k_4\eta-\frac{|zN(v-u)|+0.5(v-u)^2}{|\eta|^2}\eta+(v-u), & |\eta|\geq\varepsilon\\ 0, & |\eta|<\varepsilon,\end{cases} \tag{9}$$

where adjustable parameters $k_i>0, i=1,\cdots,4$ and $k_4>0.5(1+k_3)$. $N>1$ and $\varepsilon>0$ is a small design parameter.

The stability and convergence analysis of the closed-loop system consisting of (3) and (5)–(9) is briefly described as follows. The system (3) with the error transformation (7) and $e_2(t)=\dot{\theta}_r-\omega$ can be redescribed as

$$\begin{cases}\dot{\xi}=\frac{1}{\varphi}(e_2-\dot{\varphi}\xi)\\ b\dot{e}_2=-v(t)+a_1\theta+a_{2^+}\left(\frac{1+\mathrm{sgn}(\omega)}{2}\right)\omega+a_{2^-}\left(\frac{1-\mathrm{sgn}(\omega)}{2}\right)-a_3+a_4\mathrm{sgn}(\theta-\theta_0)+a_5\mathrm{sgn}(\omega)+\bar{T}_L+b\ddot{\theta}_r+(v-u)\end{cases} \tag{10}$$

A candidate for the Lyapunov function is chosen as follows with $\tilde{\Theta}=\Theta-\hat{\Theta}$, $\Theta=[a_1,a_{2^+},a_{2^-},a_3,a_4,a_5,b,\bar{T}_L]^T$:

$$V=\frac{1}{2}\xi^2+\frac{b}{2}z^2+\frac{1}{2}\eta^2+\frac{1}{2}\tilde{\Theta}^T\Gamma^{-1}\tilde{\Theta}, \tag{11}$$

where $\Gamma=diag\{r_i\}$, $i=1,\cdots,8$. The time derivative of V along (10) is

$$\begin{aligned}\dot{V}=&\xi\tfrac{1}{\varphi}(z+\alpha-\dot{\varphi}\xi)+z(-v(t)+a_1\theta+za_{2^+}\left(\tfrac{1+\mathrm{sgn}(\omega)}{2}\right)\omega+za_{2^-}\left(\tfrac{1-\mathrm{sgn}(\omega)}{2}\right)\omega-a_3+a_4\mathrm{sgn}(\theta-\theta_0))\\&+za_5\mathrm{sgn}(\omega)+z(b(\ddot{\theta}_r-\dot{\alpha})+\bar{T}_L+(v-u))+\eta\dot{\eta}-\tilde{\Theta}^T\Gamma^{-1}\dot{\hat{\Theta}}\end{aligned} \tag{12}$$

Considering the controller (5), the virtual control law (7) and the auxiliary system (9), (12) satisfies

$$\begin{aligned}\dot{V}\leq&-k_1\xi^2+z(a_1-\hat{a}_1)\theta+z(a_{2^+}-\hat{a}_{2^+})\left(\tfrac{1+\mathrm{sgn}(\omega)}{2}\right)\omega+z(a_{2^-}-\hat{a}_{2^-})\left(\tfrac{1-\mathrm{sgn}(\omega)}{2}\right)\omega-z(a_3-\hat{a}_3)\\&+z(a_4-\hat{a}_4)\mathrm{sgn}(\theta-\theta_0)+z(a_5-\hat{a}_5)\mathrm{sgn}(\omega)+z(b-\hat{b})(\ddot{\theta}_r-\dot{\alpha})+z(\bar{T}_L-\hat{\bar{T}}_L)\\&-k_2z^2-k_3z(z-\eta)-(k_4-0.5)\eta^2-\tilde{\Theta}^T\Gamma^{-1}\dot{\hat{\Theta}}-[|zN(v-u)|-z(v-u)]\end{aligned} \tag{13}$$

Furthermore, noting that $-k_3z(z-\eta)\leq -0.5k_3z^2+0.5k_3\eta^2$ and $N>1$ and considering the adaptive laws (6), then the following inequality holds:

$$\dot{V}\leq-k_1\xi^2-(k_2+0.5k_3)z^2-(k_4-0.5-0.5k_3)\eta^2 \tag{14}$$

Choosing the adjustable parameters $k_1>0, k_2>0, k_3>0, k_4>0.5(1+k_3)$, it follows that $\dot{V}\leq 0, \forall(\xi,z,\eta,\tilde{\Theta})\neq 0$. Therefore, the closed-loop system is Lyapunov stable at $(\xi,z,\eta,\tilde{\Theta})=0$. Furthermore, according to LaSalle's invariance principle, it follows that $\xi,z,\eta,$ are convergent to zero. Moreover, due to $0\leq\xi(t)<1$ resulting from the

transformation error $\xi(t)=e(t)/\varphi(t)$ and the definition of $\varphi(t)$, it follows that $e(t)$ can monotonically converge to zero and the entire curve of $e(t)$ is limited to $0\leq e(t)<\rho(t), \forall t\geq 0$ if $e(0)>0$ and $-\rho(t)<e(t)\leq 0, \forall t\geq 0$ if $e(0)<0$, which means that there is no overshoot in the monotonically transient response of $e(t)$.

4. Simulation verification

For safe and effective practical application in experimental platforms, the simulation results in Matlab/Simulink are first given to validate the effectiveness of the designed controller. The electronic throttle system established in Matlab/Simulink is the dynamical model (1) with (2), and the physical parameters are the parameters identified by Li and Jiao [13] for a real electronic throttle in the HIL test platform.

In simulation, the adjustable parameters of the controller are selected as follows:

$$\rho_0=1.6, \rho_\infty=0.02, \lambda=90, k_1=1, k_2=k_3=k_4=10, N=2.$$

The initial parameters of the adaptive laws are chosen as

$$\hat{a}_1(0)=0.2615, \hat{a}_{2^+}(0)=0.6158, \hat{a}_{2^-}(0)=0.6158, \hat{a}_3=0.0541, \hat{a}_4=1.2, \hat{a}_5=0.8536, \hat{\bar{T}}_L=1.5, \hat{b}=0.006.$$

The adaptive adjustable gains are selected as

$$r_1=1, r_2=10, r_3=10, r_4=100, r_5=10, r_6=5, r_7=5000, r_8=20.$$

The following four available operating cases in the simulation environment are considered to demonstrate the response performance of the resulting closed-loop systems.

Case 1: A single step signal, shown as the dashed line in Figure 2, is selected as the reference signal to observe the transient response speed of the control system.

Case 2: A group of conventional acceleration/constant deceleration processes, shown as the dashed line in Figure 3, are selected as the reference signal.

Case 3: A group of sinusoidal signals, as shown by the dashed line in Figure 4, are selected as the reference signal.

Case 4: A group of rapid acceleration/constant rapid decelerations, shown as the dashed line in Figure 5, are selected as the reference signal.

For the robustness verification, external load disturbance $\bar{T}_L=1.5+0.1\sin(2\pi t)$ and 10% perturbation of the system parameters are considered in each operating case.

Note that in practice the valve angle of the electronic throttle is only measurable; thus the feedback velocity in the controller is replaced by the estimate $\hat{\omega}=(\sigma s/(\beta s+1))\theta$, where s is the Laplace variable, β is a small number (chosen as 0.01), and the constant σ is the gain of the filter (chosen as 0.001) [1].

The simulation results, including the throttle opening, control input voltage, and tracking error, in the four cases are shown in Figures 2–5. The adaptive updating parameter curves are only given in Case 1 (see Figure 6) because the dynamical variation in the adaptive parameters in Case 1 with short time scale can be obviously displayed; this case is representative of all of the cases.

To facilitate the analysis of the simulation operation results, the transient and steady-state performance—including settling time t_s, overshoot $\sigma_p\%$, and the maximum absolute steady-state error $|e_{ss}|$ in four cases—is summarized in Table 2.

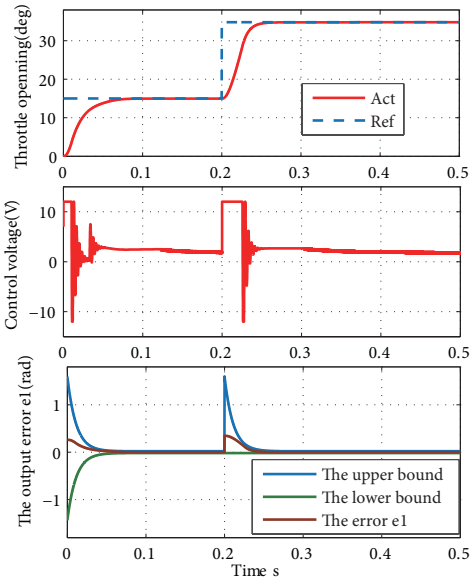

Figure 2. Throttle output and input of simulation in Case 1.

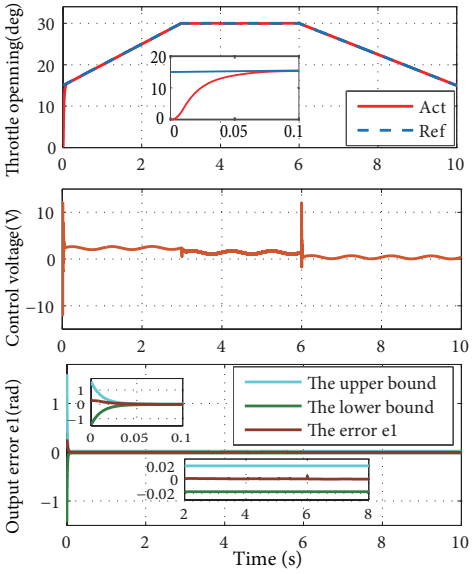

Figure 3. Throttle output and input of simulation in Case 2.

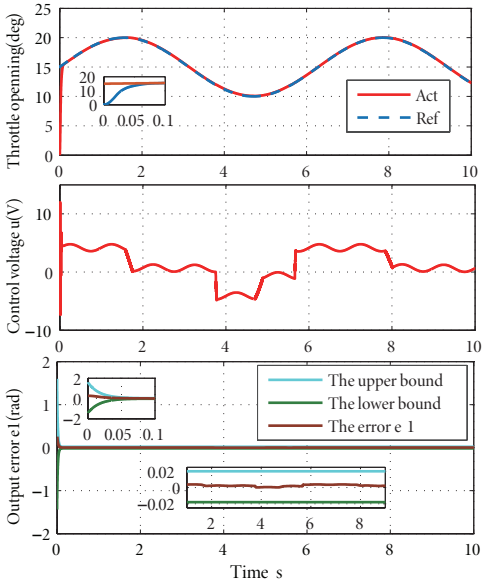

Figure 4. Throttle output and input of simulation in Case 3.

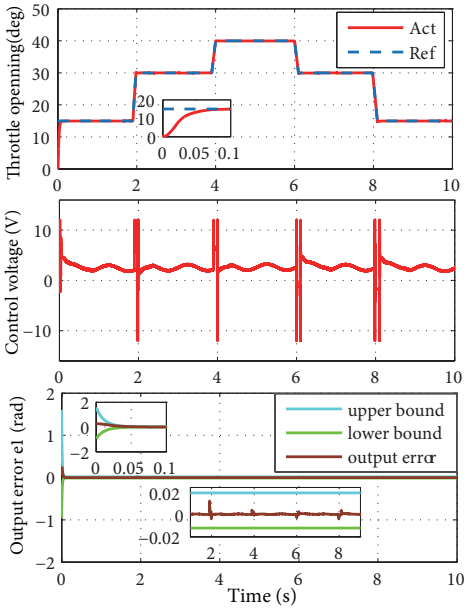

Figure 5. Throttle output and input of simulation in Case 4.

From Figures 2–6 and Table 2, it can be seen that the system error is always limited between the upper and lower limits of the performance function during the whole running process, and has satisfying transient response with no overshoot and fast settling time, while the steady-state error does not exceed ρ_∞. Moreover, the controller voltage is always limited to ± 12V during the entire operation of the four operating conditions. Meanwhile, the curves shown for $\hat{a}_1$, $\hat{a}_{2+}$, $\hat{a}_{2-}$, $\hat{a}_3$, $\hat{a}_4$, $\hat{a}_5$, $\hat{b}$, and $\hat{\bar{T}}_L$ demonstrate the adjustability and

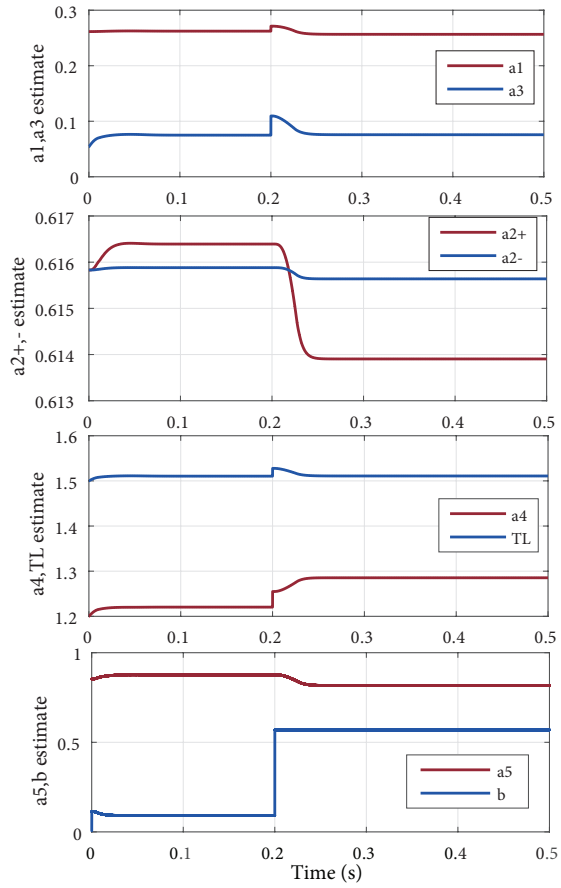

Figure 6. Adaptive parameters of simulation in Case 1.

Table 2. Transient and steady-state performance in four cases.

Case	Ref.[deg]	t_s[ms]	σ_p%[-]	e_{ss}[deg]
1	15–35 up	90	0	0.2
2	15–30 up	80	0	0.4
	30–15 down	76	0	0.3
3	15–20 up	69	0	0.3
4	15–30 up	65	0	0.2
	30–40 up	62	0	0.2
	40–30 down	55	0	0.3
	30–15 down	52	0	0.2

the boundedness with convergence to certain constants following the different operating points of adaptive parameters.

To further illustrate the effect of the adaptive update laws, we now design a prescribed performance servo controller without adaptive estimate in the following form for the nominal case of the system (3):

$$v=b\ddot{\theta}_r+a_1\theta+a_{2+}\left(\frac{1+\mathrm{sgn}(\omega)}{2}\right)\omega+a_{2-}\left(\frac{1-\mathrm{sgn}(\omega)}{2}\right)\omega-a_3+a_4\mathrm{sgn}(\theta-\theta_0)+a_5\mathrm{sgn}(\omega)-b\dot{\alpha}+\frac{\xi(t)}{\varphi(t)}+k_2z+k_3(z-\eta) \quad (15)$$

with (7)–(9). Then the comparison between the adaptive prescribed performance servo controller and the prescribed performance servo controller without adaptive estimate is given in the two cases of step signal and trapezoid signal. Moreover, the load torque with disturbance $\bar{T}_L = 1.5 + 0.1\sin(2\pi t)$ and 10% perturbation of the system parameters is considered in each operating case. The comparison results are shown in Figures 7 and 8, respectively. Obviously, from Figures 7 and 8, especially the partial enlarged figures, it can be seen that the control with adaptive law is superior to the control without adaptive estimate in both rapidity of transient response and steady-state error. The comparison results are summarized in Table 3.

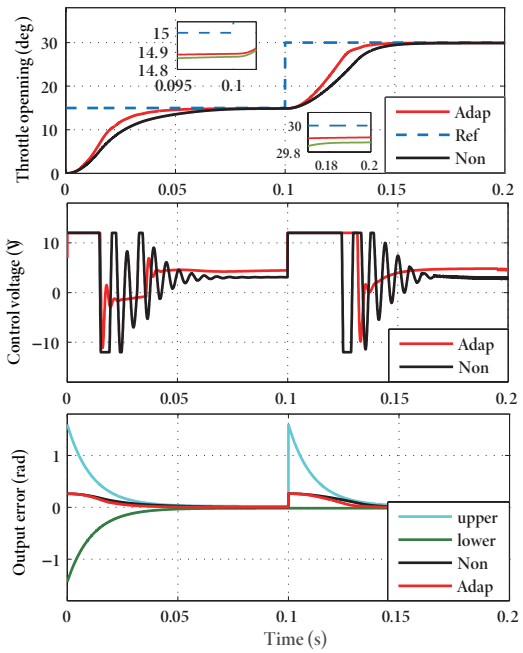

Figure 7. Simulation comparison result in step signal.

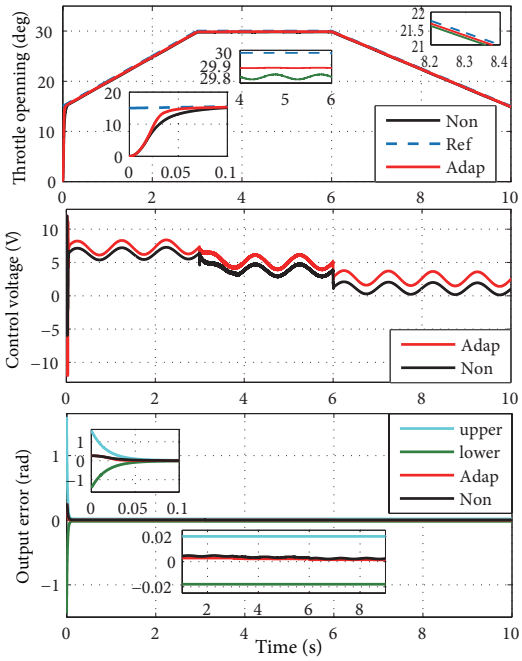

Figure 8. Summarized comparison results of the two strategies.

Table 3. Summarized comparison results of the two strategies.

Case	Signal[deg]	Strategy	t_s[ms]	σ_p%[-]	e_{ss}[deg]
1 (Figure 7)	0–15 step	adaptive	50	0	0.10
		nonadap	60	0	0.13
	15–30 step	adaptive	43	0	0.09
		nonadap	50	0	0.12
2 (Figure 8)	trapezoid	adaptive	50	0	0.13
		nonadap	62	0	0.20

5. Experiment tests

To verify the transient rapidity and steady-state accuracy, the tracking error is limited to the prescribed area in practice and the designed controller is implemented in the HIL test platform of a real ETCS, as shown in Figure 9.

Without loss of generality, the following three operating cases are considered in the experiment:

Case 1. Step signals with large angle variation in a very short time to validate the fast transient performance, shown by the dashed line in Figure 10.

Case 2. A series of smaller amplitude periodical rapid change signals to validate the ability to restrain the influence of nonlinearity on the transient performance, shown by the dashed line in Figure 11.

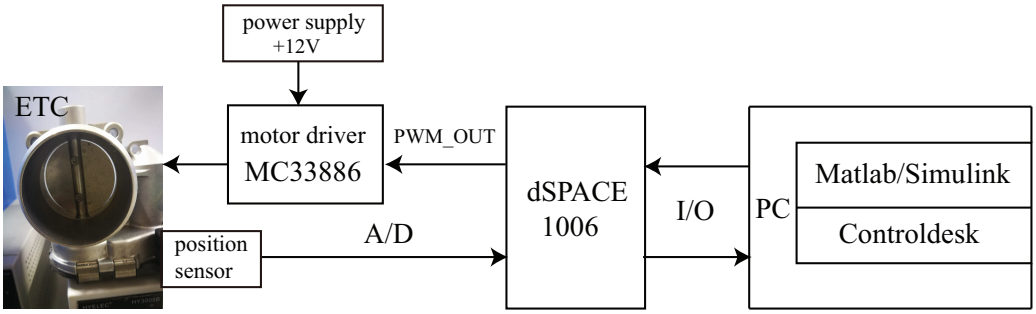

Figure 9. HIL test platform of ETCS.

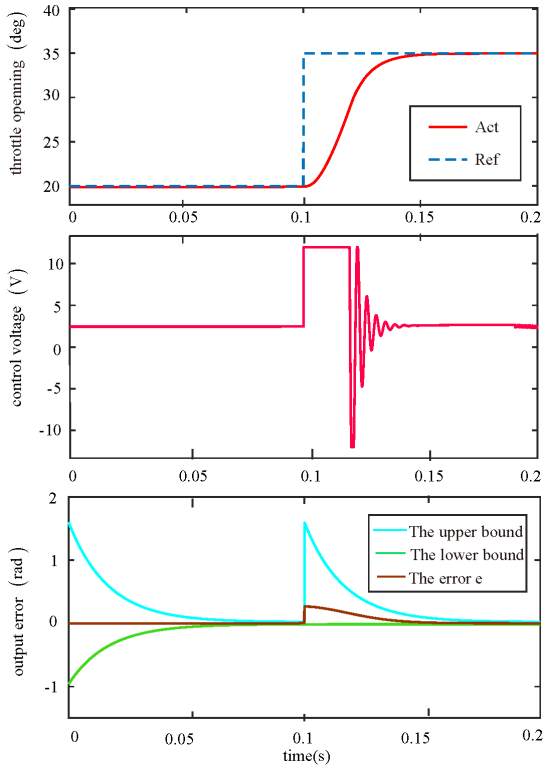

Figure 10. Experimental result in Case 1.

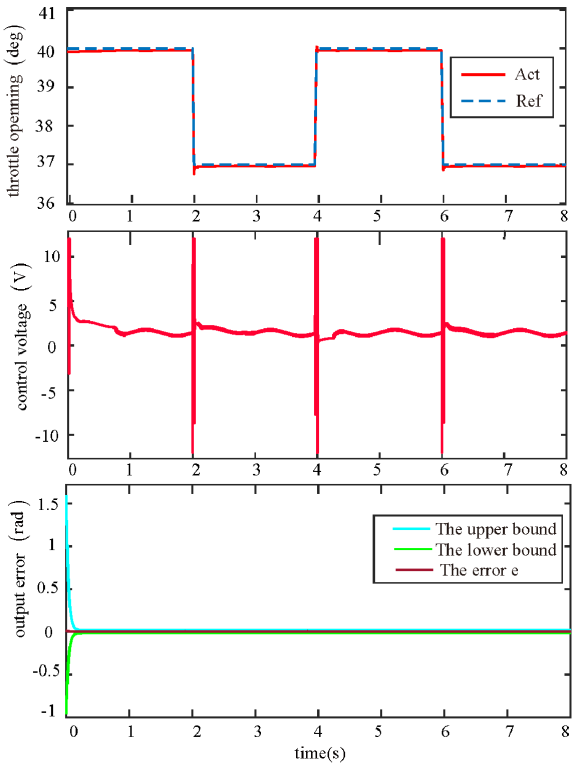

Figure 11. Experimental result in Case 2.

Case 3. A series of larger amplitude periodical rapid change signals to validate the responsiveness to larger angle variation, shown by the dashed line in Figure 12.

In the experimental test, several adjustable parameters of the controller are modified as follows: $k_1 = 20.5, k_2 = 35, r_1 = 10, r_2 = 30, r_5 = 15, r_8 = 30$. The other controller parameters are not changed. Moreover, the

load torque with disturbance and parameter perturbation considered in the experiment is also not changed.

The throttle opening and control voltage of the experimental results in the three cases are shown in Figures 10–12, and the adaptive parameters curves in Case 3 are shown in Figure 13. It can be seen from the experimental results that the designed control strategy can make the throttle valve plate quickly and accurately track the desired signal in the case of large or small angle change. The adaptive parameters can converge to some constants under different working conditions. This indicates that the proposed control scheme can achieve throttle opening tracking with satisfying transient and steady-state performance in actual operating cases.

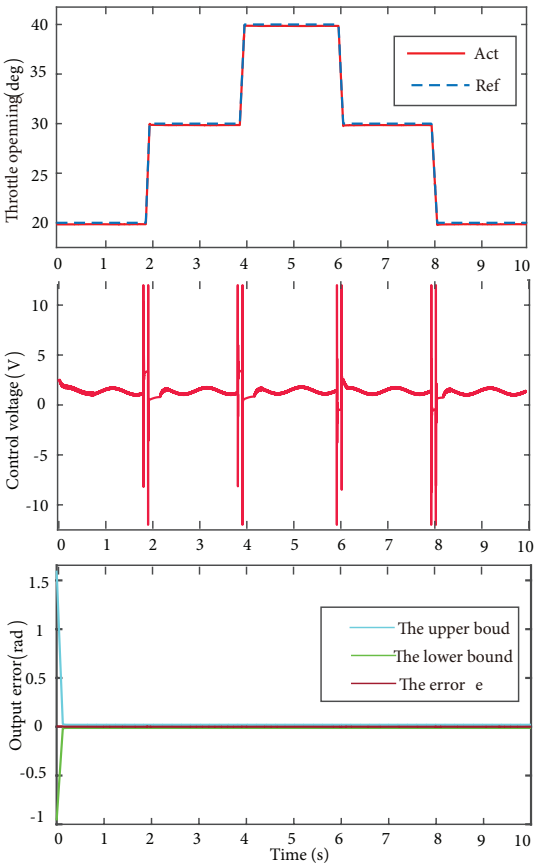

Figure 12. Experimental result in Case 3.

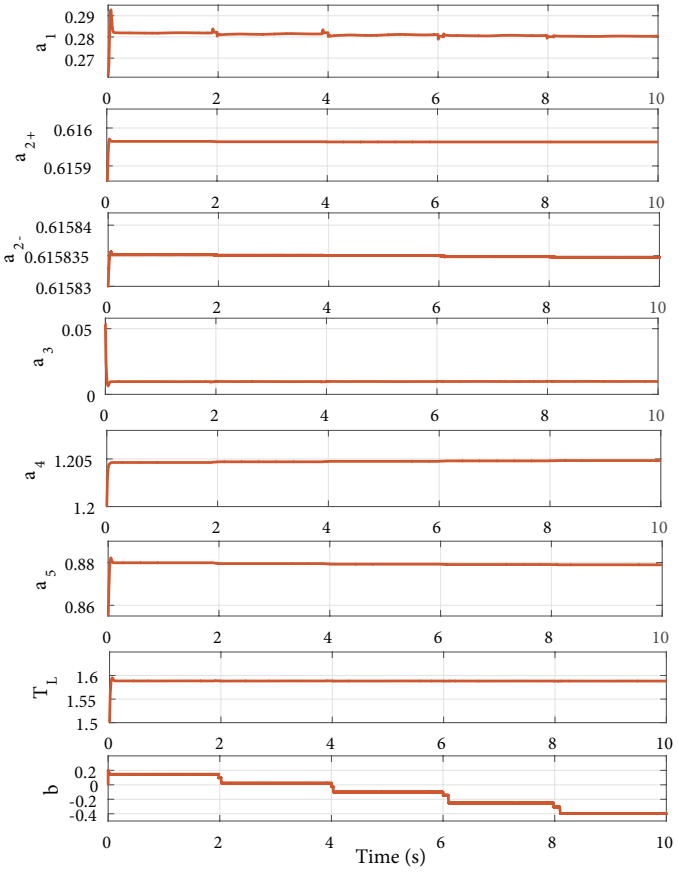

Figure 13. Adaptive parameters of experimental Case 3.

Similarly, the comparison with the prescribed performance controller without adaptive estimate is given in the two cases of larger and smaller amplitude step signals in the experiment. In all of the controller's parameters, the disturbance and parameter perturbation considered are not changed. The comparison results are shown in Figures 14 and 15. The experimental results further illustrate that the control with adaptive law is better than that without adaptive estimate in rapidity of transient response and steady-state error.

6. Conclusion

To achieve better transient and steady-state performance of the ETCS in practice, the main difficulty lies in the influence of its strong nonlinearity, parameter uncertainty, and input saturation on the control performance. Therefore, an adaptive prescribed performance control strategy with treatment of saturation, which includes a

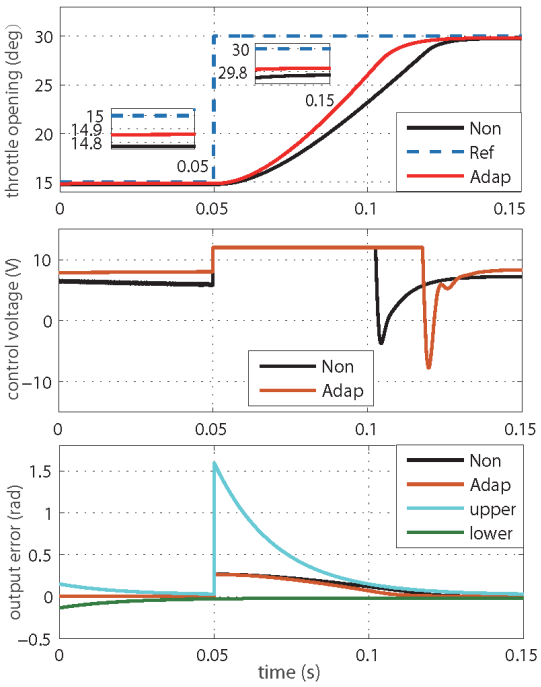

Figure 14. Experimental comparison result in larger amplitude step signals.

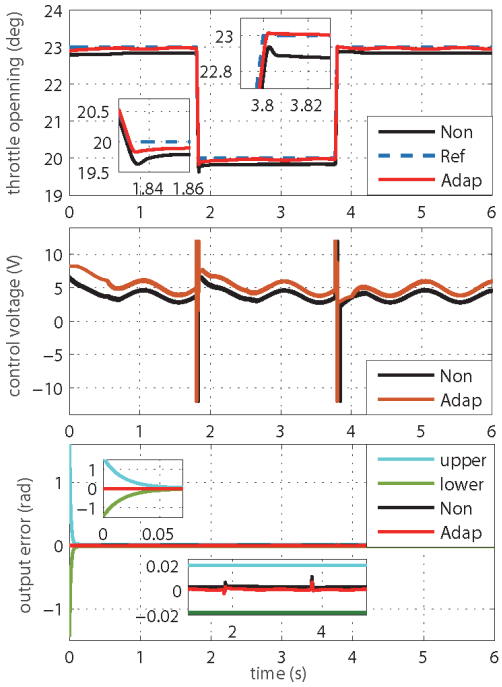

Figure 15. Experimental comparison result in smaller amplitude step signals.

prescribed performance controller, an adaptive feedforward compensation, adaptive nonlinearity compensation, and an auxiliary design system, has been given to ensure fast transient response with no overshoot and tracking error precision. An adaptive law is introduced to automatically adjust the controller's parameters corresponding to uncertain parameters. More importantly, the tracking error is between the upper and lower limits of the performance function. It should be pointed out that the initial conditions of the conversion error have a great influence on the steady-state error and transient response of the system. Simulation and experimental results show that the proposed control strategy is effective when tracking different reference signals and is robust to various changes in the operating process parameters and load disturbances.

Acknowledgment

This work was supported by the National Natural Science Foundation of China (No. 61573304) and the Natural Science Foundation of Hebei Province (Grant No. F2017203210).

References

[1] Jiao X, Zhang J, Shen T. An adaptive servo control strategy for automotive electronic throttle and experimental validation. IEEE Transactions on Industrial Electronics 2014; 61 (11): 6275-6284. doi: 10.1109/TIE.2014.2311398

[2] Montanaro U, Gaeta AD, Giglio V. Robust discrete-time MRAC with minimal controller synthesis of an electronic throttle body. IEEE/ASME Transactions on Mechatronics 2014; 19 (2): 524-537. doi: 10.1109/TMECH.2013.2247614

[3] Pavkovic D, Deur J, Jansz M, Pericet N. Adaptive control of automotive electronic throttle. Control Engineering Practice 2006; 14 (2): 121-136. doi: 10.1016/j.conengprac.2005.01.006

[4] Pujol G, Gaeta Y, Montanaro L, Vargas AN. Asymmetric modelling and control of an electronic throttle. International Journal of Numerical Modelling Electronic Networks Devices and Fields 2010; 29 (2): 192-204. doi: 10.1002/jnm.2063

[5] Yuan XF, Wang YN, Sun W, Wu L. RBF networks-based adaptive inverse model control system for electronic throttle. IEEE Transactions on Control Systems Technology 2010; 18 (3): 750-756. doi: 10.1109/TCST.2009.2026397

[6] Bai R. Adaptive sliding-mode control of an automotive electronic throttle in the presence of input saturation constraint. IEEE/CAA Journal of Automatica Sinica 2018; 5 (4): 116-122. doi: 10.1109/JAS.2018.7511147

[7] Wang H, Li ZG, Jin XZ, Huang Y, Kong H et al. Adaptive integral terminal sliding mode control for automobile electronic throttle via an uncertainty observer and experimental validation. IEEE Transactions on Vehicular Technology 2018; 67 (9): 8129-8143. doi: 10.1109/TVT.2018.2850923

[8] Wang H, Liu LF, He P, Yu M, Do TM et al. Robust adaptive position control of automotive electronic throttle valve using PID-type sliding mode technique. Nonlinear Dynamics 2013; 85 (2): 1331-1344. doi: 10.1007/s11071-016-2763-8

[9] Sun H, Zhao H, Huang K, Qiu M, Zhen S et al. A fuzzy approach for optimal robust control design of an automotive electronic throttle system. IEEE Transactions on Fuzzy Systems 2018; 26 (2): 694-704. doi: 10.1109/TFUZZ.2017.2688343

[10] Wang CH, Huang DY. A new intelligent fuzzy controller for nonlinear hysteretic electronic throttle in modern intelligent automobiles. IEEE Transactions on Industrial Electronics 2013; 60 (6): 2332-2345. doi: 10.1109/TIE.2012.2193861

[11] Yuan XF, Wang YN. A novel electronic-throttle-valve controller based on approximate model method. IEEE Transactions on Industrial Electronics 2009; 56 (3): 883-890. doi: 10.1109/TIE.2008.2004672

[12] Jiao X, Li G, Wang H. Adaptive finite time servo control for automotive electronic throttle with experimental analysis. Mechatronics 2018; 53 (4): 192-201. doi: 10.1016/j.mechatronics.2018.06.010

[13] Li G, Jiao X. Synthesis and validation of finite time servo control with PSO identification for automotive electronic throttle. Nonlinear Dynamics 2017; 90: 1165-1177. doi: 10.1007/s11071-017-3718-4

[14] Chen M, Ge SS, Ren BB. Adaptive tracking control of uncertain MIMO nonlinear systems with input constraints. Automatica 2011; 47 (3): 452-465. doi: 10.1016/j.automatica.2011.01.025

[15] Wen CY, Zhou J, Liu ZT, Su H. Robust adaptive control of uncertain nonlinear systems in the presence of input saturation and external disturbance. IEEE Transactions on Automatic Control 2011; 56 (7): 1672-1678. doi: 10.1109/TAC.2011.2122730

[16] He W, Dong YT, Sun CY. Adaptive neural impedance control of a robotic manipulator with input saturation. IEEE Transactions on Systems, Man, and Cybernetics: Systems 2016; 46 (3): 334-344. doi: 10.1109/TSMC.2015.2429555

[17] Perez-Arancibia NO, Tsao TC, Gibson JS. Saturation-induced instability and its avoidance in adaptive control of hard disk drives. IEEE Transactions on Control Systems Technology 2010; 18 (2): 368-382. doi: 10.1109/TCST.2009.2018298

[18] Han SI, Lee JM. Improved prescribed performance constraint control for a strict feedback non-linear dynamic system. IET Control Theory Applications 2013; 7 (14): 1818-1827. doi: 10.1049/iet-cta.2013.0181

[19] Wang W, Huang JS, Wen JY. Prescribed performance boundbased adaptive path-following control of uncertain nonholonomic mobile robots. International Journal of Adaptive Control Signal Processing 2017; 31 (5): 805-822. doi: 10.1002/acs.2732

[20] Na J, Chen Q, Ren XM, Guo Y. Adaptive prescribed performance motion control of servo mechanisms with friction compensation. IEEE Transactions on Industrial Electronics 2014; 61 (1): 486-494. doi: 10.1109/TIE.2013.2240635